Theor Appl Genet (2013) 126:1151–1165
DOI 10.1007/s00122-013-2043-7

ORIGINAL PAPER

Targeted linkage map densification to improve cell wall related QTL detection and interpretation in maize

Audrey Courtial · Justine Thomas · Matthieu Reymond · Valérie Méchin · Jacqueline Grima-Pettenati · Yves Barrière

Received: 21 August 2012 / Accepted: 9 January 2013 / Published online: 30 January 2013

Abstract Several QTLs for cell wall degradability and lignin content were previously detected in the F288 × F271 maize RIL progeny, including a set of major QTLs located in bin 6.06. Unexpectedly, allelic sequencing of genes located around the bin 6.06 QTL positions revealed a monomorphous region, suggesting that these QTLs were likely "ghost" QTLs. Refining the positions of all QTLs detected in this population was thus considered, based on a linkage map densification in most important QTL regions, and in several large still unmarked regions. Re-analysis of data with an improved genetic map (173 markers instead of 108) showed that ghost QTLs located in bin 6.06 were then fractionated over two QTL positions located upstream and downstream of the monomorphic region. The area located upstream of bin 6.06 position carried the major QTLs, which explained from 37 to 59 % of the phenotypic variation for per se values and extended on only 6 cM, corresponding to a physical distance of 2.2 Mbp. Among the 92 genes present in the corresponding area of the B73 maize reference genome, nine could putatively be considered as involved in the formation of the secondary cell wall [*bHLH, FKBP, laccase, fasciclin, zinc finger C2H2-type* and *C3HC4-type* (*two genes*), *NF-YB*, *and WRKY*]. In addition, based on the currently improved genetic map, eight QTLs were detected in bin 4.09, while only one QTL was highlighted in the initial investigation. Moreover, significant epistatic interaction effects were shown for all traits between these QTLs located in bin 4.09 and the major QTLs located in bin 6.05. Three genes related to secondary cell wall assembly (*ZmMYB42*, *COV1-like*, *PAL-like*) underlay QTL support intervals in this newly identified bin 4.09 region. The current investigations, even if they were based only on one RIL progeny, illustrated the interest of a targeted marker mapping on a genetic map to improve QTL position.

Communicated by T. Luebberstedt.

Electronic supplementary material The online version of this article (doi:10.1007/s00122-013-2043-7) contains supplementary material, which is available to authorized users.

A. Courtial · J. Thomas · Y. Barrière (✉)
INRA, Unité de Génétique et d'Amélioration des Plantes Fourragères, 86600 Lusignan, France
e-mail: yves.barriere@lusignan.inra.fr

A. Courtial · J. Thomas · J. Grima-Pettenati
Laboratoire de Recherche en Sciences Végétales, UMR 5546, Université de Toulouse, UPS, BP 42617, Auzeville, 31326 Castanet-Tolosan, France

A. Courtial · J. Thomas · J. Grima-Pettenati
CNRS; UMR 5546, BP 42617, 31326 Castanet-Tolosan, France

M. Reymond · V. Méchin
INRA, Institut Jean-Pierre Bourgin, 78026 Versailles, France

Introduction

Since nearly 50 years, researches have been conducted to improve the digestibility (or degradability) of the lignocellulosic cell walls of forage crops to increase their energy value in ruminants' feeding. The currently decreasing reserves of fossil fuels facing the constant needs of people and industry for energy have more recently stimulated a crucial interest in finding alternative and renewable energy resources. Lignocellulose feedstock could significantly contribute to a sustainable supply of fuels (and also chemicals), including the bioconversion of plant cell walls into bioethanol or biogas. The corresponding industrial processes generally begin by physical and/or chemical pre-

treatment(s) to break down the recalcitrant structures of the lignified cell wall material. If technological improvements of pretreatments are essential to enhance enzymatic hydrolysis of cell walls, breeding plants with increased susceptibility of their cell walls to enzymatic hydrolysis is also an effective strategy. Both technological and genetic improvements represent complementary ways towards commercializing profitable and environmentally friendly lignocellulosic bioethanol. Most forage plants are grasses, either C4 photosynthesis plants such as maize and other Panicoïdeae, or C3 plants such as ryegrass or fescue. For cellulose-based bioethanol or methane production, in addition to cropping plants of the Panicoïdeae family (maize, sorghum, switchgrass, etc.), straw of grain cereals is also a significant resource which does compete with human or animal nutrition. Despite the importance of plants of the grass family first for cattle feeding, and now for bioenergy production, most studies related to genetics, genomics, and biochemistry of cell walls and lignins have been performed on dicotyledonous species, including the *Arabidopsis* model system. This latter situation results from the use since a long time of cellulose from trees in the paper pulping industry, and more recently because woody biomass and byproducts are a large resource for lignocellulosic bioenergy.

The grass cell wall is a specific composite material including phenolic compounds, cellulose microfibrils, and an amorphous matrix consisting predominantly of glucurono-arabinoxylans. Phenolic compounds are composed of lignins and cell wall linked *p*-hydroxycinnamates, *p*-coumaric (*p*CA), and ferulic (FA) acid derivatives. Grass lignins include guaiacyl (G) units derived from coniferyl alcohol, syringyl (S) units derived from sinapyl alcohol, together with *p*-hydroxyphenyl units (H) derived from *p*-coumaryl alcohol. The low, but appreciable amount of H units, nearly five times higher than in dicotyledonous plants, significantly impacts the properties of grass cell walls as these units increase the frequency of resistant inter-unit bonds. The participation of *p*-hydroxycinnamates in the lignified cell wall is specific to grass species, and this gives its original structure and properties. In the grass cell wall, a large proportion of S units are acylated by *p*CA, and extensive cross-linkages occur between feruloylated arabinoxylans and G units of lignins, as well as between arabinoxylan chains after ferulate dimerization in mature cell walls (Ralph et al. 1992, 1995; Jacquet et al. 1995; Grabber et al. 2004; Ralph 2010). Lignins are essential for structural integrity of tissues and they impart hydrophobicity to vascular elements. Their association with other matrix components, together with the occurrence of linkages with and between cell wall carbohydrates, significantly impedes tissue properties towards higher stiffness and lower polysaccharide degradability, with negative effects on silage energy value and also on bioethanol or biogas production.

In addition, large ranges of genetic variation for cell wall degradability were shown in maize, opening ways for an efficient breeding for silage and/or for biofuel production (Dhillon et al. 1990; Lundvall et al. 1994; Barrière et al. 2004a; Andersen et al. 2007; Riboulet et al. 2008; Barrière et al. 2009). Cell wall degradability is the result of the combined effects of the cell wall composition in phenolic compounds as well as of the structural organization of lignified tissues. Therefore, the identification of genes involved in secondary wall formation and assembly deserves priority interest for maize biomass quality improvement. In addition, plant breeders have to choose cell wall trait combinations for minimizing negative effects on genotype agronomic value, including whole plant yield, standability, biotic, and abiotic stress tolerance.

The characterizations of maize mutants and/or of genetically engineered plants have highlighted a few genes capable of affecting maize cell wall degradability. It is the case of genes involved in monolignol biosynthesis (*CAD*, *COMT*, *CCR*; Vignols et al. 1995; Halpin et al. 1998; He et al. 2003; Barrière et al. 2004b; Pichon et al. 2006; Tamasloukht et al. 2011) as well as transcription factors of the MYB family regulating lignin biosynthesis (*ZmMYB31*, *ZmMYB42*; Fornalé et al. 2006, 2010; Sonbol et al. 2009). However, the involvement of these genes in the natural variation in degradability between maize lines has not yet been established. In addition, the observed cell wall degradability improvements in these mutants often occurred together with negative effects on plant agronomic value. Efficient breeding of maize with higher cell wall degradability for silage use or second-generation bioethanol production therefore demands the identification of the major determinants driving traits under selection. The search for candidate genes underlying QTLs for cell wall degradability and related traits is thus a relevant strategy for further key-gene discovery and consequently efficient marker-assisted selection. QTLs for cell wall-related traits have been mostly detected in maize (reviewed in Barrière et al. 2007, 2009 and references therein; Barrière et al. 2010, 2012) and to a lesser extent in woody species such as pine (Sewell et al. 2002; Markussen et al. 2003; Pot et al. 2006), poplar (Yin et al. 2010), and *Eucalyptus* (Freeman et al. 2009; Thumma et al. 2010; Gion et al. 2011). However, no gene has yet been identified as being responsible for the effect of any cell wall QTL, even if co-localizations between candidate genes and QTLs were found in maize, *Arabidopsis*, poplar, and *Eucalyptus* (Barrière et al. 2010; Ranjan et al. 2010; Thomas et al. 2010; Gion et al. 2011; Chavigneau et al. 2012). This is mainly due to our limited understanding of the major genetic determinants of cell wall biosynthesis and assembly, even if exhaustive lists of

candidate genes involved either in the biosynthesis of phenolic compounds or in the formation and assembly of secondary walls as well as in the regulation of these processes have been proposed (Barrière et al. 2009; Chavigneau et al. 2012). The frequent large size of the QTL support intervals, with an average length of 20 cM corresponding to 15–50 Mbp according to genomic location and recombination rate, is the second reason which renders the identification and validation of candidate genes difficult.

In the F288 × F271 early maize RIL progeny, several QTLs were previously mapped, of which those located in bin 6.06 explained a highly significant part of the phenotypic variation for both lignin content and cell wall degradability, with R^2 values ranging from 20 to 40 % (Roussel et al. 2002; Thomas et al. 2010). However, the support intervals of these QTLs represented more than 20 cM, which corresponded to nearly 12 Mbp and more than 800 genes in the B73 reference genome. Allelic variation of putative candidate genes in bin 6.06 was investigated as a preliminary step towards the identification of the possible involvement of these genes in the effect of the detected QTLs. Simultaneously, linkage map densification was performed to (1) reduce the size of QTL support intervals, (2) to investigate whether the large effect QTLs corresponded to a single major QTLs or to closely linked QTLs with lower effects, and then to (3) identify putative candidate genes taking advantage of the maize B73 genomic sequence (Schnable et al. 2009, http://www.maizesequence.org, release v2 5b60) and information on gene physical positions. New markers were therefore targeted within the QTL support intervals, together with a marker densification on the whole F288 × F271 genetic map.

Materials and methods

RIL production and RIL experiments

The set of 131 RILs was developed by single seed descent from the cross between the two early dent inbred lines F288 and F271 at INRA Lusignan, France (Barrière et al. 2001). F271 and F288 have low and medium–high cell wall degradability, respectively. F271 and F288 lines have both a Co125 common ancestry [F271 = (Co125 × W103), F288 = (F244 × F252) with F244 = (F186 × F188) and F252 = (F186 × Co125)]. As reported in Roussel et al. (2002), RIL progenies were evaluated in field experiments for their per se values in seven environments (two locations over 3 years, and 1 year with an extra location), and for topcross experiments with F286 as flint tester of high cell wall degradability line in six environments (three locations over 2 years). Topcross and RILs per se were evaluated in generalized alpha-lattice designs with, in each location, three replicates for the tested RILs and nine replicates for the parents. Each experimental plot was a 5.2 m long single row of 37 plants. Row spacing was 0.75 m, and the resulting density was 95,000 plants/ha. Irrigation was applied in Lusignan during summer to prevent water stress. At the silage harvest stage [about 30–35 % of whole plant dry matter (DM)], the plots were machine-harvested with a forage chopper. A representative sample of 1 kg chopped material per plot was collected for further analyses.

A highly significant genetic variation was shown for two lignin content and two cell wall digestibility traits, which all had high broad sense heritability values (Roussel et al. 2002). Lignin content was first estimated as ADL/NDF. According to Goering and van Soest (1970) neutral detergent fiber (NDF) is an estimate of cell wall content, and acid detergent lignin (ADL) is an estimate of lignin content. Lignin content was also estimated as Klason lignin (KL) according to Dence and Lin (1992). KL includes an acido-soluble part of lignin which is lost during the first step of the ADL procedure (Hatfield et al. 1994; Jung et al. 1997; Hatfield and Fukushima 2005). Given that grain is much more digestible than cell walls, and because starch content must be limited in ruminant diets to avoid acidosis risks, cell wall digestibility traits free of starch content were considered. In vitro NDF digestibility (IVNDFD) is thus an estimate of cell wall digestibility, based on the enzymatic solubility of Aufrère and Michalet-Doreau (1983), which is computed according to Struik (1983) and Dolstra and Medema (1990), assuming that the non-NDF part is fully digestible. In vitro digestibility of the non-starch, non-soluble carbohydrates, non-crude protein part (DINAGZ) is another estimate of cell wall digestibility, similarly based on the same enzymatic solubility, which is computed according to Argillier et al. (1995) and Barrière et al. (2003), assuming that starch, crude proteins, and soluble carbohydrates are fully digestible. The corresponding individual RIL per se and topcross mean values over locations obtained by Roussel et al. (2002) for ADL/NDF, KL/NDF, IVNDFD, and DINAGZ were used as phenotypic values in the present QTL investigation.

Allele sequencing

Genomic DNA was isolated from young maize leaves of F271 and F288 lines using the DNeasy Plant mini kit (Qiagen). Primer pairs were designed on the B73 genomic sequence (Schnable et al. 2009, http://www.maizesequence.org, release v2 5b60) to generate an amplicon of nearly 1,000 base pair, using primer 3 software (http://www.frodo.wi.mit.edu/primer3/ and Supplementary table 1). PCR amplification reactions were performed in

25 µl containing 1× buffer, 4 % DMSO, 200 µM of each dNTP, 0.2 µM of each 5′ oligo and 3′ oligo, and 0.5 U of Platinum Taq Polymerase (Invitrogen, 10966); 30 ng of genomic DNA was used as template. The PCR cycling program consisted of an initial denaturation of 2 min at 94 °C, followed by 40 cycles for 30 s at 94 °C, 30 s at 60 °C, and 1 min at 72 °C, and a final extension for 5 min at 72 °C. Sequencing was performed for each of the PCR fragments in both directions by the Millegen Company (31670 Labège, France). All the sequences were aligned with the B73 sequence using the CLUSTALX2 software.

Genotypic data and development of a new linkage map

The linkage map of the F288 × F271 RIL progeny was originally drawn based on 108 SSR markers and 131 RILs (Barrière et al. 2001). New markers were added with a targeted strategy not only to increase the marker density in the most important QTL regions, especially in bin 6.06, but also to set markers in several large still unmarked regions. New considered markers were first 113 SSR markers available in the MaizeGDB database (http://www.maizegdb.org) with unambiguous physical positions. In addition, 128 new markers were designed specifically in genes chosen for physical positions and preferentially considering genes involved in cell wall biosynthesis, according to the list proposed by Barrière et al. (2009). Primer pairs were designed based on the B73 genomic sequence (Schnable et al. 2009, http://www.maizesequence.org) using primer 3 software (sequences available upon request). Genotyping was also reinvestigated for six SSR markers present on the original map, but with missing data or discrepancies between genetic and physical positions. Finally, three SSR markers available from investigations performed in 2001 (Barrière et al. 2001), but not yet included in the published genetic map, were added to the renewed map.

Gene and marker polymorphisms were analyzed with high-resolution melting (HRM) technology using the LightCycler 480 system (Roche Applied system). Genomic DNA was isolated from young maize leaves of the two parental F271 and F288 lines and of each RIL cropped at INRA, Lusignan (France), except for a few RILs for which DNA was directly isolated from grain after observation of their null or poor germination (adapted protocol from Dellaporta and Hicks 1983). Heterozygous DNA was produced by extracting DNA from fresh F288 and F271 mixture plant material. HRM polymorphisms were first revealed on the DNA from parental lines and this heterozygote DNA. If convenient results were obtained, markers were genotyped on the whole RIL progeny using the two F288 and F271 lines, and the constructed heterozygote as melting standard. PCR amplification reactions were performed in 10 µl containing 1× buffer, 200 µM of each dNTP, 0.2 µM of each primer, 4 % DMSO, 3 mM MgCl2, 0.15 unit of Platinum Taq DNA Polymerase (Invitrogen, 10966), and 0.25 × ResoLight (Roche Diagnostics, 0490964000). Approximately 20 ng of genomic DNA was used as template. The PCR cycling program consisted of 5 min at 94 °C, followed by 50 cycles for 30 s at 94 °C, 1 min at 60 °C, and 1 min at 72 °C. The HRM reaction was performed for 1 min at 95 °C, cooling to 40 °C for 1 min, raising the temperature to 65 °C, and then to 95 °C with 25 fluorescent acquisitions per Celsius degree at this step. The following data analysis was performed with the gene scanning software module on the LightCycler® 480 instrument. The linkage map was developed using CarthaGene (version 1.2.2, De Givry et al. 2005).

QTLs identification and candidate genes

QTL detection was then performed following the method of composite interval mapping (CIM, Zeng 1994) implemented in the PLABQTL software (Utz and Melchinger 1996) as previously performed by Roussel et al. (2002). PLABQTL uses the regression method (Haley and Knott 1992) in combination with markers which are selected by stepwise regression as cofactors. LOD support intervals are constructed in PLABQTL according to Lander and Botstein (1989) and are considered to be underestimated in the case of CIM. The percentage of phenotypic variance ascribed to an individual QTL was estimated with the approximate standard error of Kendall and Stuart (1961). The additive effects of QTL were estimated as half the difference between the phenotypic values of the respective homozygotes. Based on the permutation-test method of Churchill and Doerge (1994), LOD thresholds equal to, respectively, 3.0, 3.5, and 4.6 allowed an experiment-wise error rates equal to 10, 5, and 1 %. QTLs were finally considered for LOD thresholds higher or equal to 3.0, to highlight most of them. In addition, QTLs with lower LOD values were also considered when they were shown in colocalizing positions. Detection of epistatic interactions has been performed with R software using the scan two procedure of the QTL library as described by Broman and Sen (2009). Physical QTL positions were estimated based on physical positions of the two flanking markers (B73 line sequence, release v2 5b60), assuming a linear relationship between recombination and physical distances within this interval. The lists of genes underlying QTLs were established according to the filtered gene set genes presented in the same reference genome (Maize Sequence database, Schnable et al. 2009).

Results

Allele sequencing reveals ghost QTLs in bin 6.06

Allele sequencing was first carried out for genes putatively involved in cell wall biosynthesis within the bin 6.06 region where lignin content and cell wall degradability QTLs with high R^2 values were located (Roussel et al. 2002; Thomas et al. 2010), (i.e. from 149.4 to 164.5 Mbp; Table 1). Genomic sequence of three candidate genes considered of priority interest were full-length sequenced (nearly 500 bp before ATG and after stop codons), including the *cinnamate-3-hydroxylase C3H2* (GRMZM2G140817) involved in monolignol biosynthesis, the *MYB Hv5-like* (GRMZM2G077789) which is a R2R3 MYB repressor orthologous to barley *Hv5 MYB* genes (Wissenbach et al. 1993) and to *EgMYB1* (Legay et al. 2007, 2010; Grima-Pettenati et al. 2012), and the continuous vascular ring *COV1-like* (GRMZM2G101533), ortholog of an *Arabidopsis* gene involved in lignified tissue patterning (Parker et al. 2003). Twenty-one other candidate genes were only partially sequenced (over 1,000 bp length). No allelic polymorphism between the two parental lines F271 and F288 was found for the two fully sequenced *C3H2* and *COV1-like* genes (position 155.7 and 159.8 Mbp, respectively). In addition, all other ten investigated genes located between the *zinc finger C3HC4* (GRMZM2G157246, position 155.2 Mbp) and the *OsIAA18-like* (GRMZM2G074427, position 160.2 Mbp), including these two genes, were also monomorphic between the two parental lines. In contrast, the ten investigated genes located upstream the *zinc finger C3HC4*, including the *MYB Hv5-like*, were polymorphic between F271 and F288. Similarly, downstream of the *OsIAA18-like* gene, the MYB *AtMYB26-like* (GRMZM2G175232, position 162.1 Mbp) was polymorphic. However, the sequence of the downstream *NAC SND2/SND3-like* (GRMZM2G031200, position 164.5 Mbp) gene was identical between both parental lines. As a tentative conclusion, no polymorphism was revealed in a 5 Mbp long region (12 investigated genes within this region), corresponding to nearly 50 % of the QTL support interval and overlapping all QTLs estimated positions (based on the data of Roussel et al. 2002). This region was therefore considered as monomorphic between the two parental lines, and consequently, detected QTLs at this locus were considered as putative "ghost" QTLs. Map densification, and generating a new linkage map, in this major QTL region, as well as in areas with low marker density, was therefore an obligatory step to precise QTL positions.

Revisiting of the polymorphism between F288 and F271 and generating a new linkage map

We tested 247 new markers of which 114 (46 %) were polymorphic between the two parental lines, 94 (38.0 %) were monomorphic, and 39 (16 %) failed during the HRM assay. Finally, 75 new polymorphic markers were analyzed on the whole RIL progeny, including the six re-investigated markers. The still unused three SSR markers genotyped in 2001 were added to the map, whereas seven markers, which failed to be relevantly added to linkage groups during the map construction, were removed. The new map (Fig. 1) was significantly densified with 173 markers as compared to the original map established in 2001 which only contained 108 SSR markers.

The new map, which spans a cumulative distance of 2,153 cM, shows an average distance between markers of 13.2 cM while it was 22.3 cM long on the 2001 map. Distances between markers were, however, unevenly distributed, with the smallest distances equal to 0.4 cM, while the largest ones were greater than or equal to 60 cM. Differences between chromosomes and between areas resulted both from the focus given on some areas, and also from the absence of polymorphic marker on other areas. Two large gaps, more than 60 cM long, were still present on chromosome 7, which likely correspond to large monomorphic areas. A similar situation was shown on chromosome 10 for which the first marker of the 2001 map (bnlg2190) was located in physical position 141.8 Mbp. The current investigations allowed to map mmc0501 at the upstream part of chromosome 10, in position 5.9 Mbp. Between the two markers mmc0501 and bnlg2190, only four markers out of the 34 tested were found to be polymorphic, one in position 8.8 Mbp and three surrounding the position 125 Mbp. These results strengthened a large monomorphic area of nearly 110 Mbp long on chromosome 10.

QTL detection

Overall, based on the new linkage map, 43 QTLs were detected for lignin content (ADL/NDF, KL/NDF) and cell wall degradability (DINAGZ, IVNDFD) traits in the F288 × F271 progeny for both per se and topcross experiments (Table 2), while only 32 were found in 2001. QTLs were distributed on nine chromosomes (since no QTL was detected on chromosome 10) and 17 genomic positions. Co-localizations between QTLs were observed on most positions, and only five QTLs were found in isolated positions, on chromosomes 4 (2 QTLs), 5, 7, and 8. A similar number of QTLs were mapped using data from per se (20 QTLs) and topcross (23 QTLs) experiments. Five QTLs were detected for ADL/NDF in per se experiments and six in topcross experiments. Four and six KL/NDF QTLs were detected for per se and topcross values, respectively. Eight QTLs for DINAGZ were observed for per se values and four for topcross values. Finally, three and seven IVNDFD QTLs were detected for per se and topcross values, respectively. Marker densification of the

Table 1 Polymorphism of putative lignin-related candidate genes underlying bin 6.06 QTLs

Markers, genes and QTLs	Gene name	Bin	Phys pos	F288/F271	
				SNP	InDel
bnlg1702 (120.2 cM)		6.05	147.1	–	–
NAC domain-containing protein	GRMZM2G465835	6.05	149.4	**0**	**1**
Continuous vascular ring like (LCV2-like)	GRMZM2G073415	6.05	150.3	**5**	**0**
F288 × F271 QTL upper limit (150.0 cM)		6.05	150.4	–	–
MYB Hv5-like EgMYB1-like R2R3-type[a]	GRMZM2G077789	6.05	150.7	**8**	**4**
Zinc finger C3HC4 transcription factor	GRMZM2G066225	6.05	150.8	**10**	**3**
bHLH transcription factor	GRMZM2G061906	6.05	151.1	**21**	**2**
ZmLac6 AtLac17 ortholog	GRMZM2G146152	6.05	151.5	**na**	**na**
Zinc finger C2H2 transcription factor	AC206217.2_FGT006	6.05	151.8	**3**	**12**
Zinc finger C3HC4 transcription factor	GRMZM2G075782	6.05	152.8	**na**	**na**
Zinc finger C3HC4 transcription factor	GRMZM2G035601	6.05	152.9	**1**	**0**
WRKY transcription factor OsWRKY70-like	GRMZM2G169966	6.05	153.3	**24**	**9**
bnlg345 (177.2 cM)		6.05	153.5	–	–
Zinc finger Ring H2 transcription factor	GRMZM2G390436	6.06	154.2	**8**	**6**
MYB transcription factor SHAQKYF class	GRMZM2G701218	6.06	155.2	**19**	**6**
Zinc finger C3HC4 transcription factor	GRMZM2G157246	6.06	155.2	*0*	*0*
MYB transcription factor SHAQKYF class	GRMZM2G117854	6.06	155.5	*0*	*0*
Cytochrome P450 CYP98A1 (C3H2)[a]	GRMZM2G140817	6.06	155.7	*0*	*0*
CCAAT-HAP5 transcription factor	GRMZM2G440949	6.06	155.7	*na*	*na*
Zinc finger C2H2 transcription factor	GRMZM2G159741	6.06	156.0	*0*	*0*
bZIP transcription factor	GRMZM2G175870	6.06	156.0	*0*	*0*
F288 × F271 QTL position (181.7 cM)		6.06	156.1	–	–
Zinc finger CCCH transcription factor	AC226373.2_FGT010	6.06	156.4	*0*	*0*
Ras small GTPase ROP6-like	GRMZM2G176217	6.06	158.4	*na*	*na*
Auxin response factor 4 (ARF)	GRMZM2G441325	6.06	158.7	*0*	*0*
ZRP4-like OMT	GRMZM2G140996	6.06	158.7	*0*	*0*
ZRP4-like OMT	GRMZM2G141026	6.06	158.7	*0*	*0*
ZRP4-like OMT	GRMZM2G102863	6.06	158.8	*na*	*na*
ZRP4-like OMT	GRMZM2G124799	6.06	158.8	*na*	*na*
Continuous vascular ring (COV1-like)[a]	GRMZM2G101533	6.06	159.8	*0*	*0*
WRKY transcription factor OsWRKY58-like	GRMZM2G401521	6.06	159.8	*0*	*0*
Auxin-responsive Aux/IAA OsIAA18-like	GRMZM2G074427	6.06	160.2	*0*	*0*
ZmMYB AtMYB26-like	GRMZM2G175232	6.07	162.1	**7**	**8**
F288 × F271 QTL lower limit (198.0 cM)		6.07	162.6	–	–
WD40 repeat-like	GRMZM2G038032	6.07	162.9	**na**	**na**
NAC SND2/SND3-like	GRMZM2G031200	6.07	164.5	*0*	*0*
phi089 (213.4 cM)		6.07	166.3	–	–

Markers and genes with polymorphism are shown in bold, and those without detected polymorphism are shown in italics

na unavailable data

[a] Full length gene sequencing

genetic map allowed us to pinpoint several QTL positions and to reduce the support intervals of QTLs.

Only 8 QTLs out of 43 explained less than 10 % of the observed genetic variation (LOD < 3.00), while 4 QTLs explained more than 30 % of the observed variation. These major QTLs co-localized in bin 6.05, a little upstream of the revealed monomorphic region. Moreover, QTLs for all investigated traits in both per se and topcross experiments were observed in this region, except for the KL/NDF trait in topcross experiments. QTLs located in bin 6.05 explained from 37 to 59 % of the observed variation for lignin content and cell wall degradability in per se experiments, whereas the topcross QTLs explained only 8–12 % of the observed variation. These QTLs are all located in

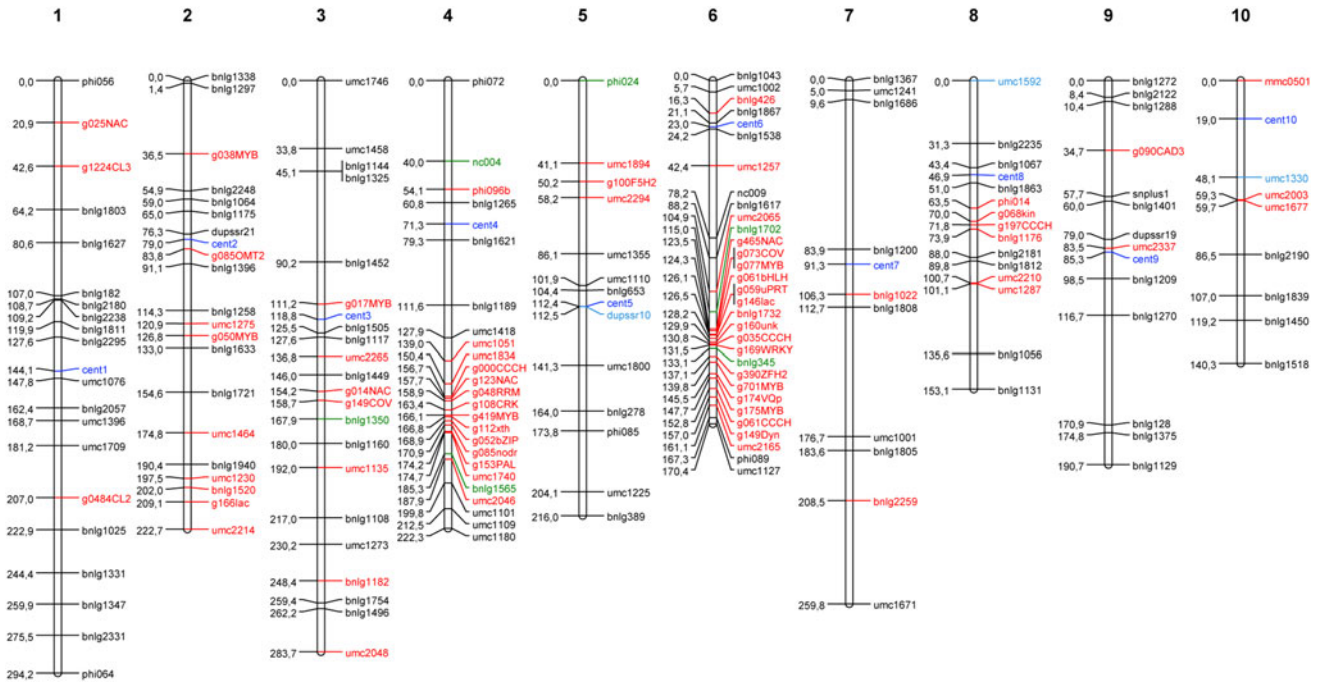

Fig. 1 New linkage map of the F288 × F271 RIL progeny with 173 makers (*Black* markers correspond to markers mapped on the previous map with 108 markers (Barrière et al. 2001), *red* markers to markers newly genotyped in 2011, *light blue* markers to markers genotyped in 2001 but not included in the previously published map, *green* markers to re-genotyped marker (2001 data replaced by 2011 data). Centromere (cent) positions were estimated based on physical positions in B73. Names on the *right* of the chromosome correspond to SSR names or gene names (abbreviated from GRMZM2G identifier followed by gene annotation). *Numbers* on the *left* of the chromosome indicate marker positions in cM from the *top* of the chromosome)

support intervals from 126 to 130 cM (bin 6.05), except the per se value KL/NDF QTL found slightly downstream, between 128 and 132 cM. Downstream of this region and of the monomorphic area, topcross QTLs were also shown for all traits in position 148 cM (bin 6.07), except for KL/NDF QTL detected in position 142 cM. The latter position was still unexpected as it corresponded to the so-called monomorphic area. Downstream QTLs explained from 9 to 16 % of the genetic variation. Finally, the seven "ghost" QTLs shown in 2001 in bin 6.06 likely corresponded to QTLs located in two positions, one upstream for both per se and topcross values (bin 6.05, position 151.8 Mbp), and one downstream for topcross values (bin 6.07, position 162.1 Mbp), even if one was still located in the monomorphic area (Fig. 2). Based on the 2001 map, bin 6.06 QTLs expanded over a 48 cM long support interval corresponding to 12.2 Mbp (150.4–162.6 Mbp). Based on the current map, QTLs only span over a 6 cM long interval corresponding to 2.2 Mbp (151.1–153.3 Mbp) for the upstream position, and only over 4 cM corresponding to a little more than 1.2 Mbp (151.1–152.3) if the little downstream KL/NDF QTL was not considered. For the downstream QTL position, QTLs span over a 10 cM long interval corresponding to 3.7 Mbp (159.2–162.9 Mbp, when excluding the KL/NDF topcross QTL still located in the monomorphic area).

In addition, eight QTLs were detected on chromosome 4, in bin 4.09, following the map densification (13 new markers) and reassessment in this region (Fig. 3). Only one QTL, explaining 9 % of the DINAGZ variation, was found in 2001. These newly detected QTLs were distributed in three successive non-overlapping regions. QTLs with the highest R^2 values (ranging between 15 and 26 %) after those observed in bin 6.05 were co-localized in one of these regions. This region extended over 10 cM, corresponding to 17 Mbp (216.4–233.3 Mbp). Furthermore, significant epistatic interactions were detected between QTLs in bin 6.05 (average position 129 cM) and QTLs in bin 4.09 (166 cM) for all traits in per se and in topcross experiments. These epistatic interactions revealed that, in addition to the main effects of both major QTLs located on chromosomes 6 and 4, the effects of the QTLs on chromosome 6 were more pronounced when alleles from F271 were present at QTL positions on chromosome 4 (Fig. 4, illustrating epistatic interactions for ADL/NDF and IVNDFD traits in per se experiments).

Candidate genes underlying bins 6.05, 6.07, and 4.09 QTLs

Ninety-two genes were present under the 2.2 Mbp support interval of QTLs located in bin 6.05. This gene number was

Table 2 QTL analysis for cell wall investigated traits in the F288 × F271 RIL progeny, based on the 173 marker map and on Roussel et al. (2002) phenotypic data

QTL	Chrom	Bin	Pos	Left_Mark	Supp.IV	LOD	R2	Add	Line +
KL/NDF tc	1	1.01	26	g025NAC	14–38	3.24	10.8	−0.117	F271
KL/NDF ps	1	1.01	32	g025NAC	24–42	5.74	18.3	−0.385	F271
DINAGZ ps	1	1.01	36	g025NAC	24–52	3.40	11.3	0.509	F288
IVNDFD tc	1	1.08	242	bnlg1025	230–254	3.28	10.9	−0.292	F271
KL/NDF tc	1	1.09	250	bnlg1331	230–260	3.00	10.1	0.114	F288
IVNDFD ps	2	2.08	194	bnlg1940	178–198	2.12	7.2	0.579	F288
KL/NDF tc	2	2.08	196	bnlg1940	190–202	4.54	14.8	−0.126	F271
ADL/NDF ps	2	2.08	198	umc1230	192–204	5.36	17.2	−0.166	F271
DINAGZ ps	2	2.09	200	umc1230	196–206	3.59	11.9	0.443	F288
ADL/NDF tc	2	2.09	202	umc1230	198–206	5.59	17.8	−0.071	F271
IVNDFD tc	2	2.09	202	umc1230	198–206	5.88	18.7	0.360	F288
DINAGZ tc	3	3.05	124	g017MYB	116–128	2.33	7.9	0.189	F288
DINAGZ ps	3	3.05	124	g017MYB	116–128	2.82	9.4	0.493	F288
ADL/NDF tc	3	3.05	134	bnlg1117	126–146	3.57	11.8	−0.060	F271
DINAGZ ps	3	3.06	142	umc2265	136–152	2.29	7.7	0.512	F288
IVNDFD tc	3	3.06	152	bnlg1449	144–160	4.03	13.2	0.309	F288
ADL/NDF tc	4	4.09	158	g123NAC	156–160	2.83	9.5	−0.049	F271
IVNDFD tc	4	4.09	158	g123NAC	156–160	4.16	13.6	0.296	F288
IVNDFD ps	4	4.09	168	g112xth	166–172	5.27	16.9	0.878	F288
KL/NDF ps	4	4.09	168	g112xth	166–172	5.79	18.4	−0.309	F271
ADL/NDF ps	4	4.09	168	g112xth	166–172	6.25	19.7	−0.180	F271
KL/NDF tc	4	4.09	168	g112xth	166–170	8.51	25.9	−0.169	F271
DINAGZ ps	4	4.09	174	g153PAL	170–176	4.62	15.0	0.528	F288
DINAGZ ps	4	4.09	198	umc2046	192–204	3.74	12.5	0.543	F288
ADL/NDF ps	5	5.08	210	umc1225	188–216	3.90	13.8	0.163	F288
DINAGZ ps	6	6.01	20	bnlg426	16–26	5.46	17.5	0.547	F288
ADL/NDF ps	6	6.01	22	bnlg1867	16–26	2.00	6.8	−0.099	F271
ADL/NDF tc	6	6.05	128	g146lac	126–130	2.38	8.0	−0.055	F271
IVNDFD tc	6	6.05	128	g146lac	126–130	2.99	10.0	0.318	F288
DINAGZ tc	6	6.05	128	g146lac	126–130	3.60	11.9	0.289	F288
ADL/NDF ps	6	6.05	128	g146lac	126–130	13.46	37.7	−0.308	F271
DINAGZ ps	6	6.05	128	g146lac	126–130	18.10	47.1	1.321	F288
IVNDFD ps	6	6.05	128	g146lac	126–130	25.04	58.5	2.533	F288
KL/NDF ps	6	6.05	130	g160unk	128–132	13.16	37.0	−0.576	F271
KL/NDF tc	6	6.06	142	g701MYB	136–146	5.08	16.3	−0.140	F271
DINAGZ tc	6	6.07	148	g175MYB	144–154	2.51	8.5	0.216	F288
ADL/NDF tc	6	6.07	148	g175MYB	144–152	4.05	13.3	−0.068	F271
IVNDFD tc	6	6.07	148	g175MYB	144–152	4.31	14.1	0.354	F288
ADL/NDF tc	7	7.03	190	bnlg1805	176–204	3.03	10.1	−0.063	F271
DINAGZ tc	8	8.04	66	phi014	56–70	5.08	16.4	0.289	F288
KL/NDF ps	9	9.03	86	umc2337	78–94	4.48	14.6	0.296	F288
IVNDFD tc	9	9.03	86	umc2337	80–94	5.47	17.5	−0.390	F271
KL/NDF tc	9	9.03	94	umc2337	86–112	5.04	16.2	0.141	F288

IVNDFD, in vitro neutral detergent fiber digestibility; DINAGZ, in vitro cell wall digestibility according to Argillier et al. (1995); ADL/NDF, acid detergent lignin/neutral detergent fiber; KL/NDF, Klason lignin/NDF; in per se (ps) and topcross (tc) experiments. Positions given as cM

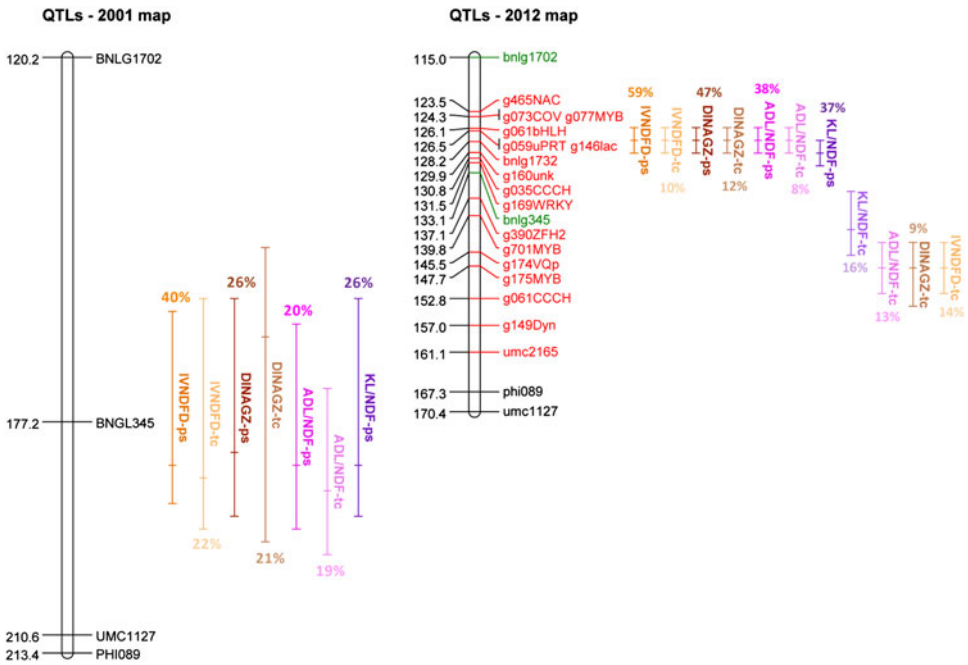

Fig. 2 Improvement of cell wall related QTL positions in the bin 6.06 of the 131 RIL F288 × F271 progeny. Comparison of QTL detection based on 2001 linkage map (*left* chromosome) and 2012 current linkage map (*right* chromosome) [Abbreviations and legends as in Table 2 and Fig. 1. *Numbers* on the *left* of the chromosome indicate genetic position in cM from the *top* of the chromosome. Percentages under or above QTL *bars* correspond to R^2 values]

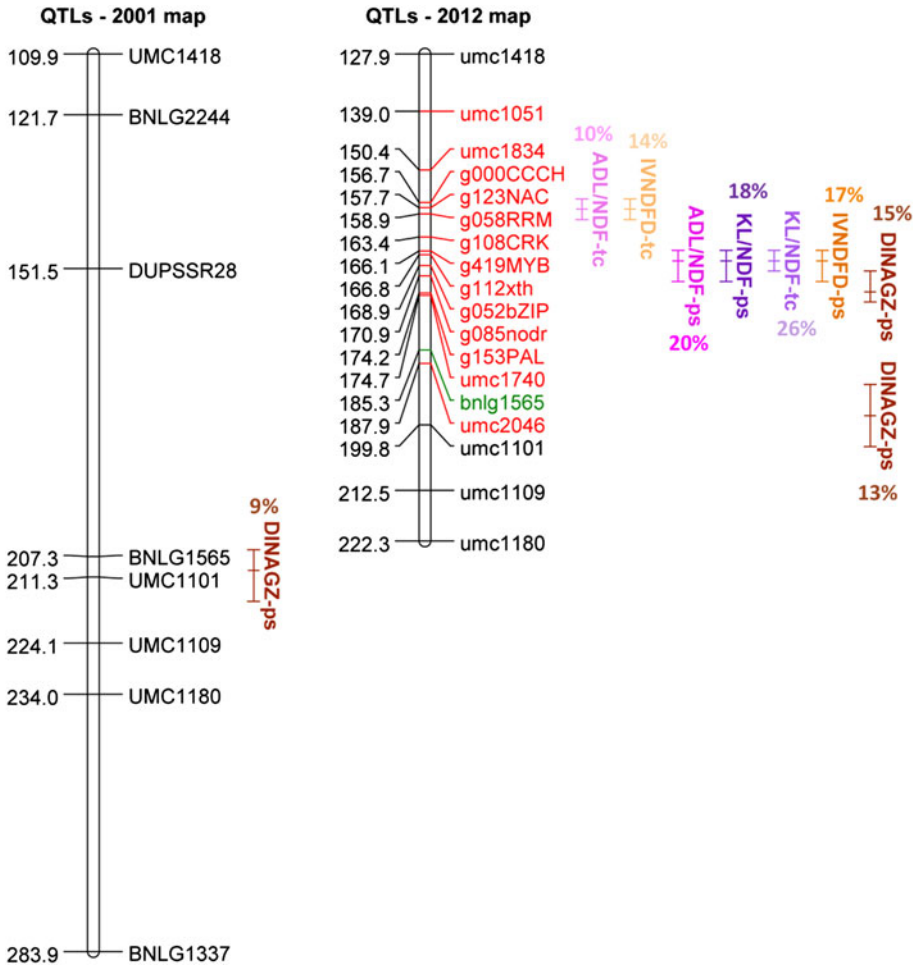

Fig. 3 Improvement of cell wall related QTL positions in bin 4.09 of the F288 × F271 RIL progeny. Comparison of QTL detection based on 2001 linkage map (*left* chromosome) and on current 2012 linkage map (*right* chromosome) [Abbreviations and legends as in Table 2 and Fig. 1. *Numbers* on the *left* of the chromosome indicate genetic position in cM from the *top* of the chromosome. Percentages under or above QTL *bars* correspond to R^2 values]

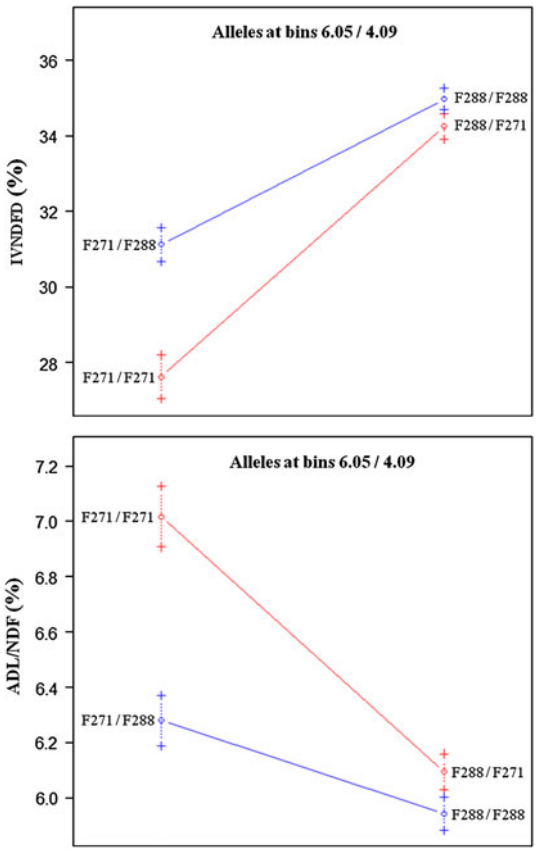

Fig. 4 Epistatic interactions between QTLs located in bins 6.06 and 4.09 for ADL/NDF and IVNDFD traits

lowered to 50 genes if the little downstream KL/NDF QTL was not considered. Nearly 800 genes were present in the region highlighted in 2001. According to the MapMan BIN classification (Thimm et al. 2004), 39 % of the 92 currently considered genes have an unknown function. Among genes with functional annotations, only nine were known to belong to families with members (putatively) related to the secondary cell wall assembly (*bHLH*, *FKBP*, *laccase*, *fasciclin*, one *zinc finger C2H2* and two *zinc finger C3HC4*, *NF-YB*, and *WRKY*). The *bHLH* (GRMZM2G061906), located in position 151.3 Mbp, is an ortholog of the *AtbHLH105* (At5g54680) transcription factor *ILR3* (Pires and Dolan 2010). While the role of ILR3 in secondary wall assembly is not established, other bHLH proteins were shown to be involved in the regulation of the phenyl propanoid metabolism (Heim et al. 2003; Ramsay and Glover 2005). The *FK506-binding proteins* (*FKBPs*) gene (GRMZM2G035922), located in position 151.5 Mbp, is an ortholog of *AtFKBP20-1* (At3g55520), a gene belonging to the large family of peptidyl–prolyl *cis–trans* isomerases. These genes are known to be involved in growth and development (Harrar et al. 2001), based on observations in several mutants such as *pasticcino1* (*pas1*) and *twisted dwarf* (*twd*). Moreover, the *FKBPs* gene was less expressed in four RILs of the F288 × F271 progeny, with both the favorable allele and high cell wall degradability, compared to the parental line F271 with low degradability (Courtial et al. 2012). However, its possible role in constitutive lignified tissue assembly is not yet established. The *laccase* gene (GRMZM2G146152), located at 151.5 Mbp, is one ortholog of *AtLac17* (At5g60020), which is involved in monolignol polymerization in *Arabidopsis* stems (Berthet et al. 2011). Moreover, *AtLac17* co-localized with a QTL of lignin content in a RIL progeny of *Arabidopsis* (Chavigneau et al. 2012). The *fasciclin* gene (AC213621.5_FG004), located in position 151.6 Mbp, is orthologous to the *SOS5* (*Salt Overly Sensitive5*) *Arabidopsis* gene, of which mutants have thinner cell walls. This gene encodes a putative cell-surface adhesion protein which is required for normal cell expansion (Shi et al. 2003). Three *zinc finger* genes, including one zinc finger of the *C2H2-type* (AC206217.2_FG006), located in position 151.8 Mbp, and two *zinc finger* of the *C3HC4-type* (GRMZM2G075782 and GRMZM2G035601), in positions 152.8 and 152.9 Mbp, co-localized with QTLs located in bin 6.05. *Zinc finger* genes belong to one of the largest families of transcription factor regulatory proteins, which are involved in numerous regulations during plant development. The *zinc finger C2H2* family was the most frequently represented in *Eucalyptus* secondary xylem libraries (Rengel et al. 2009). *Zinc finger C3HC4* genes were the most differentially expressed transcription factors in a comparison between tension wood, with lower lignin content, and normal *Populus* wood (Andersson-Gunneras et al. 2006). Moreover, plants over-expressing C3HC4 gene have also increased cellulose and reduced lignin contents in *Eucalyptus* (Arruda and Gerhardt 2010). *Nuclear factor Y subunit B*, (GRMZM5G804893), located in position 152.2 Mbp, is an ortholog of *NF-YB8*, a gene expressed in vascular tissue of *Arabidopsis* (Siefers et al. 2009), with a still unclear role. Finally, the *WRKY* gene (GRMZM2G169966), located in position 153.3 Mbp, belongs to a large family of transcription factors involved in development or in response to environmental signals, and especially to biotic and abiotic stress response. Its *Arabidopsis* ortholog *AtWRKY33* is thus involved in defense reactions (Zheng et al. 2006).

Two genes out of the 172 genes co-localizing with the 3.7 Mbp support interval of the downstream topcross QTLs (bin 6.07) were directly related to secondary cell wall biosynthesis and assembly. The *COV1-like* gene (GRMZM2G101533), in position 159.8 Mbp, is an ortholog of an *Arabidopsis* gene involved in lignified tissue patterning (Parker et al. 2003). However, this gene did not show any polymorphism between the two parental lines F288 and F271, and was located at the basal part of the monomorphic area. The role of the *MYB*

gene (GRMZM2G175232), just flanking the QTL position (162.1 Mbp), is not yet known. However, the encoded protein has homology with the *Eucalyptus EgrMYB137* expressed in xylem tissues (Soler, com pers). It also has homology with *AtMYB26*, of which loss of function induced a defect in the secondary wall thickening of *Arabidopsis* endothecium resulting in anther indehiscence (Yang et al. 2007). These homologies could corroborate a role of this *ZmMYB* in secondary wall formation.

In addition, 513 genes were shown underlying support intervals of QTLs located in a 17 Mbp region of bin 4.09, which are epistatic to QTLs located in bin 6.05. Among these genes, three are directly related to secondary cell wall biosynthesis and assembly. The *ZmMYB42* gene (GRMZM2G419239) is a transcriptional repressor of the maize lignin pathway genes (Fornalé et al. 2006; Sonbol et al. 2009; Gray et al. 2012). The *COV1-like* (GRMZM2G123790) gene is an ortholog of the *COV1 Arabidopsis* gene, involved in the regulation of vascular patterning in the stem (Parker et al. 2003). The *PAL-like* (GRMZM2G153871) gene is paralogous to the members of the PAL family, which are involved in the first step of monolignol biosynthesis. In addition, a single base pair INDEL in the *ZmPAL* gene (GRMZM2G074604) has been associated with the in vitro degradability of organic matter of plants (Andersen et al. 2007).

Discussion

A new linkage map to revisit line polymorphism and highlight monomorphic areas

Nearly half (50.2 %) of the 494 successfully tested markers were shown to be polymorphic, which is a little more than the average of usual polymorphism rates in maize (Yan et al. 2010). However, several areas remained with large distance between polymorphic markers on the improved F288 × F271 map, corresponding to the areas for which all tested markers did not show any polymorphism. These regions were then supposed to be monomorphic between the two parental lines, likely as a consequence of the common Co125 ancestry in the two F288 and F271 lines. In addition, it was suspected that breeding efforts for grain yield in F288 and F271 have also favored Co125 alleles, and consequently induced larger monomorphic genomic areas in their progeny than expected from their lineage (Roussel et al. 2002).

Ghost QTLs in bin 6.06 correspond likely to two distinct QTLs positions

The fact that QTLs estimated positions detected in 2001 in bin 6.06 were located in a monomorphic region could result from wrong QTLs positions as a consequence of insufficient markers coverage and/or RIL number in the progeny (57 cM between bnlg1702 and bnlg345, 36.2 cM between bnlg345 and phi089, and only 131 RILs). It could also be the consequence of the joint influence of two dependent QTL positions for the investigated traits (Martinez and Curnow 1992; Studer and Doebley 2011). The addition of 17 new markers between bnlg1702 and phi089 allowed distinguishing two distinct chromosomal regions involved in cell wall degradability and lignin content, one in bin 6.05 for per se and topcross values, just upstream of the supposed monomorphic area, and another for topcross values only in bin 6.07, downstream of the supposed monomorphic area. Corroborating the two slightly different QTL positions, one QTL affecting fiber and lignin contents in stalk was detected near the 155 Mbp position in the B73 × De811 F3 progeny (Krakowsky et al. 2003), while two QTL positions were detected later near the 150 and 165 Mbp positions in the B73 × De811 RIL progeny (Krakowsky et al. 2005). Finally, ghost QTLs detected in 2001 for topcross value were thus split into two QTL positions separated by 20 cM, and situated on both sides of the previous position, confirming the joint influence of two linked QTLs. These two QTLs had quite similar R^2 values, of which the sum was close to 2001 R^2 values. The per se QTL position observed in 2001 should probably be the consequence of the low marker density of the original map in this region. In addition, several candidate genes and/or polymorphisms could be jointly responsible for the variable phenotypes observed at each QTL positions.

Other contributions of the densified map for the detection of QTLs and limits

Marker densification of the genetic map allowed to pinpoint QTL positions and to reduce support intervals of QTL, as was shown by Darvasi et al. (1993). Furthermore, new QTLs were shown in bin 4.09, a region where the two initial markers (bnlg2244 and dupssr28) were removed and replaced by 14 new or re-genotyped markers. This result highlighted the impact of marker spacing on QTL detection. The improved map allowed also reducing QTL support intervals, and consequently the number of candidate genes underlying these QTLs. However, the interval support lengths, equal to 6 and 10 cM for QTLs located in bins 6.05 and 4.09 (major and epistatic QTLs), respectively, have likely now reached their minimum sizes with seven and six markers underlying them, pointing out the limits imposed by the population size (Darvasi et al. 1993).

In addition, QTL effects were still high in these two regions. However, the estimates of phenotypic variances associated with correctly identified QTL were shown to be overestimated when the number of progenies was low

(Beavis 1998; Xu 2003). The high R^2 values observed in this experiment should thus be considered in light of the so-called Beavis effect. Nevertheless, large R^2 values could also be the consequence of multiple closely linked QTLs present under the interval support (Studer and Doebley 2011).

Conclusion

The objective of this study was to identify the candidate genes underlying the major QTLs for cell wall degradability and lignin contents previously detected in bin 6.06 in the F288 × F271 RIL progeny (Roussel et al. 2002). These QTLs expanded over a 48 cM long support interval corresponding to 12.2 Mbp, and more than 800 genes in the B73 reference genome. As a first step towards gene identification, allelic variation was investigated for putative candidate genes involved in cell wall biosynthesis and assembly. This targeted sequencing highlighted a monomorphic region between the two parental lines, including the QTL estimated positions and consequently suggested that detected QTLs were likely "ghost" QTLs. Targeted map densification, using HRM, was thus performed to pinpoint QTL positions and to reduce their support interval lengths. Markers were mapped in the most important QTLs regions, especially within or at the close vicinity of the major bin 6.06 QTLs support intervals, and in several large still unmarked regions. Finally, only few areas remained with large distance between markers, as a consequence of the absence of polymorphism in these regions, likely due to parental line consanguinity.

In the F288 × F271 progeny, 43 QTLs were detected for lignin (ADL/NDF, KL/NDF) and cell wall degradability (DINAGZ, IVNDFD) traits from both per se and topcross experiments with the improved map, while only 32 were highlighted with the map drawn in 2001. This increase in the QTL number could be explained by the fact that several large effect QTLs were fractionated in two QTLs (bin 6.06) and that new regions involved in degradability were revealed (bin 4.09). The putative ghost QTL positions in bin 6.06 indeed corresponded to two regions, with cell wall trait QTLs detected at the two positions, one located upstream (bin 6.05) and one downstream (bin 6.07) of the monomorphic area. Major per se QTLs in this progeny co-localized now in bin 6.05 with support intervals only extending on 6 cM corresponding to 2.2 Mbp. This decrease of QTL support interval lengths came along with a strong reduction of gene number underlying QTLs (currently 92 genes versus 800 genes based on 2001 map). Among these 92 genes, nine could putatively be considered as involved in the biosynthesis and the assembly of the secondary cell wall and the regulation of these processes. However, genes of unknown function, or genes for which roles in lignification have not yet been established, could be the true candidate or could belong to a group of underlying determinants.

In addition to the improvement of bin 6.06 QTL positions, new areas involved in cell wall degradability were detected after the marker densification in bin 4.09. Per se QTLs with high R^2 values co-localized in this region and showed significant epistatic interactions with the major QTLs located in bin 6.05. Three genes greatly related to secondary cell wall were present in this region (*ZmMYB42*, *COV1-like*, *PAL-like*). Finally, this study allowed refining the search for QTLs related to cell wall degradability and lignin content, and thus to fractionate large-effect QTLs, corroborating the questioning proposed by Studer and Doebley (2011). Following the length reduction of QTL support interval, the identification of the only gene or clustered genes responsible of the QTLs was simultaneously made easier, with a great reduction of gene number underlying QTL areas. The reduced support interval length also allows the establishment of BAC libraries of the two parental lines F271 and F288, followed by the targeted sequencing of BACs overlapping the corresponding QTL support intervals. The current investigations are based only on one RIL progeny, and the interest of the candidate genes underlying QTLs for breeding will need further validation on wider based germplasm. However, because no candidate gene has been discovered under any of the numerous QTLs detected for cell wall related traits, the investigations in the bins 4.09 and 6.05 of the F288 × F271 RIL progeny should provide relevant clues about the genetic determinants responsible for variation in maize and grass cell wall degradability.

Acknowledgments This work has been funded by the maize breeding companies involved in the PROMAÏS—INRA network on maize cell wall lignification and digestibility (Advanta, Caussade Semences, Limagrain Europe, MaïsAdour, Monsanto SAS, Pioneer Génétique, Pau Euralis, R2n RAGT Semences, SDME KWS France, Syngenta seeds). We thank Christiane Minault, Dominique Denoue and Pascal Vernoux for seed multiplications and plant cropping and sampling at INRA Lusignan. We also thank Jacques Laborde, who managed seed multiplications at INRA, St Martin de Hinx, France. We are grateful to Fabien Mounet for his fruitful criticisms.

References

Andersen JR, Zein I, Wenzel G, Krutzfeldt B, Eder J, Ouzunova M, Lübberstedt T (2007) High levels of linkage disequilibrium and associations with forage quality at a Phenylalanine Ammonia-Lyase locus in European maize (*Zea mays* L.) inbreds. Theor Appl Genet 114:307–319

Andersson-Gunneras S, Mellerowicz EJ, Love J, Segerman B, Ohmiya Y, Coutinho PM, Nilsson P, Henrissat B, Moritz T,

Sundberg B (2006) Biosynthesis of cellulose-enriched tension wood in *Populus*: global analysis of transcripts and metabolites identifies biochemical and developmental regulators in secondary wall biosynthesis. Plant J 45:144–165

Argillier O, Barrière Y, Hébert Y (1995) Genetic variation and selection criterion for digestibility traits of forage maize. Euphytica 82:175–184

Arruda P, Gerhardt IR (2010) Nucleic acid molecules encoding plant proteins in the C3HC4 family and methods for the alteration of plant cellulose and lignin content. US Patent App. 12/520, 266 US 2010/0077509 A1

Aufrère J, Michalet-Doreau B (1983) In vivo digestibility and prediction of digestibility of some by-products. In: EEC seminar, Melle-Gontrod, Belgium, 26–29 September, pp 25–33

Barrière Y, Gibelin C, Argillier O, Méchin V (2001) Genetic analysis and QTL mapping in forage maize based on recombinant inbred lines descended from the cross between F288 and F271. I—Yield, earliness, starch and crude protein content. Maydica 46:253–266

Barrière Y, Guillet C, Goffner D, Pichon M (2003) Genetic variation and breeding strategies for improved cell wall digestibility in annual forage crops. Rev Anim Res 52:193–228

Barrière Y, Emile JC, Traineau R, Surault F, Briand M, Gallais A (2004a) Genetic variation for organic matter and cell wall digestibility in silage maize. Lessons from a 34-year long experiment with sheep in digestibility crates. Maydica 49:115–126

Barrière Y, Ralph J, Méchin V, Guillaumie S, Grabber JH, Argillier O, Chabbert B, Lapierre C (2004b) Genetic and molecular basis of grass cell wall biosynthesis and degradability. II. Lessons from brown-midrib mutants. C R Biol 327:847–860

Barrière Y, Riboulet C, Méchin V, Maltese S, Pichon M, Cardinal AJ, Lapierre C, Lübberstedt T, Martinant JP (2007) Genetics and genomics of lignification in grass cell walls based on maize as a model system. Genes Genomes Genomics 1:133–156

Barrière Y, Méchin V, Lafarguette F, Manicacci D, Guillon F, Wang H, Lauressergues D, Pichon M, Bosio M, Tatout C (2009) Towards the discovery of maize cell wall genes involved in silage quality and capability to biofuel production. Maydica 54:161–198

Barrière Y, Méchin V, Denoue D, Bauland C, Laborde J (2010) QTL for yield, earliness and cell wall digestibility traits in topcross experiments of F838 × F286 RIL progenies. Crop Sci 50:1761–1772

Barrière Y, Méchin V, Lefevre B, Maltese S (2012) QTLs for agronomic and cell wall traits in a maize RIL progeny derived from a cross between an old Minnesota13 line and a modern Iodent line. Theor Appl Genet 125:531–549

Beavis WD (1998) QTL analyses: power, precision, and accuracy. In: Paterson AH (ed) Molecular dissection of complex traits. CRC Press, Boca Raton, pp 145–162

Berthet S, Demont-Caulet N, Pollet B, Bidzinski P, Cezard L, Le Bris P, Borrega N, Herve J, Blondet E, Balzergue S, Lapierre C, Jouanin L (2011) Disruption of LACCASE4 and 17 results in tissue-specific alterations to lignification of *Arabidopsis thaliana* stems. Plant Cell 23:1124–1137

Broman KW, Sen Ś (2009) A guide to QTL mapping with R/qtl. Springer, New York. ISBN 978-0-387-92124-2

Chavigneau H, Goué N, Courtial A, Jouanin L, Reymond M, Méchin V, Barrière Y (2012) QTL for floral stem lignin content and degradability in three recombinant inbred line (RIL) progenies of *Arabidopsis thaliana* and search for candidate genes involved in cell wall biosynthesis and degradability. OJGen 2:7–30

Churchill GA, Doerge RW (1994) Empirical threshold values for quantitative trait mapping. Genetics 138:963–971

Courtial A, Jourda C, Arribat S, Balzergue S, Huguet S, Reymond M, Grima-Pettenati J, Barrière Y (2012) Comparative expression of cell wall related genes in four maize RILs and one parental line of variable lignin content and cell wall degradability. Maydica 57:56–74

Darvasi A, Weinreb A, Minke V, Weller JI, Soller M (1993) Detecting marker-QTL linkage and estimating QTL gene effect and map location using a saturated genetic-map. Genetics 134:943–951

De Givry S, Bouchez M, Chabrier P, Milan D, Schiex T (2005) CARTHAGENE: multipopulation integrated genetic and radiated hybrid mapping. Bioinformatics 21:1703–1704

Dellaporta J, Hicks JB (1983) A plant DNA minipreparation: version II. Plant Mol Biol Rep 1:19–21

Dence C, Lin SY (1992) The determination of lignin. Methods in lignin chemistry. Springer, Berlin, pp 33–62

Dhillon B, Paul C, Zimmer E, Gurrath P, Klein D, Pollmer W (1990) Variation and covariation in stover digestibility traits in diallel crosses of maize. Crop Sci 30:931–936

Dolstra O, Medema JH (1990) An effective screening method for genetic improvement of cell-wall digestibility in forage maize. In: Proceedings 15th congress maize and sorghum section of Eucarpia, 4–8 June, Baden, pp 258–270

Fornalé S, Sonbol FM, Maes T, Capellades M, Puigdomènech P, Rigau J, Caparrós-Ruiz D (2006) Down-regulation of the maize and *Arabidopsis thaliana* caffeic acid *O*-methyl-transferase genes by two new maize R2R3-MYB transcription factors. Plant Mol Biol 62:809–823

Fornalé S, Shi X, Chai C, Encina A, Irar S, Capellades M, Fuguet E, Torres JL, Rovira P, Puigdomènech P, Rigau J, Grotewold E, Gray J, Caparrós-Ruiz D (2010) *Zm*MYB31 directly represses maize lignin genes and redirects the phenylpropanoid metabolic flux. Plant J 64:633–644

Freeman JS, Whittock SP, Potts BM, Vaillancourt RE (2009) QTL influencing growth and wood properties in *Eucalyptus globulus*. Tree Genet Genomes 5:713–722

Gion JM, Carouche A, Deweer S, Bedon F, Pichavant F, Charpentier JP, Bailleres H, Rozenberg P, Carocha V, Ognouabi N, Verhaegen D, Grima-Pettenati J, Vigneron P, Plomion C (2011) Comprehensive genetic dissection of wood properties in a widely-grown tropical tree: eucalyptus. BMC Genomics 12:301

Goering HK, Van Soest PJ (1970) Forage fiber analysis (Apparatus, reagents, procedures and some applications). US Department of Agriculture Science Handbook n°379, pp 1–20

Grabber JH, Ralph J, Lapierre C, Barrière Y (2004) Genetic and molecular basis of grass cell-wall degradability. I. Lignin-cell wall matrix interactions. C R Biol 327:455–465

Gray J, Caparrós-Ruiz D, Grotewold E (2012) Grass phenylpropanoids: regulate before using! Plant Sci 184:112–120

Grima-Pettenati J, Soler M, Camargo E, Wang H (2012) Chapter 6—transcriptional regulation of the lignin biosynthetic pathway revisited: new players and insights. In: Lise Jouanin and Catherine Lapierre (eds) Advances in botanical research, Vol 61. Academic Press, pp 173–218

Haley CS, Knott SA (1992) A simple regression method for mapping quantitative trait loci in line crosses using flanking markers. Heredity 69:315–324

Halpin C, Holt K, Chojecki J, Oliver D, Chabbert B, Monties B, Edwards K, Barakate A, Foxon GA (1998) Brown-midrib maize (bm1)—a mutation affecting the cinnamyl alcohol dehydrogenase gene. Plant J 14:545–553

Harrar Y, Bellini C, Faure JD (2001) FKBPs: at the crossroads of folding and transduction. Trends Plant Sci 6:426–431

Hatfield R, Fukushima RS (2005) Can lignin be accurately measured. Crop Sci 45:832–839

Hatfield RD, Jung HJG, Ralph J, Buxton DR, Weimer PJ (1994) A comparison of the insoluble residues produced by the Klason lignin and acid detergent lignin procedures. J Sci Food Agric 65:51–58

He X, Hall MB, Gallo-Meagher M, Smith RL (2003) Improvement of forage quality by downregulation of maize *O*-methyltransferase. Crop Sci 43:2240–2251

Heim MA, Jakoby M, Werber M, Martin C, Weisshaar B, Bailey PC (2003) The basic helix-loop-helix transcription factor family in plants: a genome-wide study of protein structure and functional diversity. Mol Biol Evol 20:735–747

Jacquet G, Pollet B, Lapierre C (1995) New ether-linked ferulic acid-coniferyl alcohol dimers identified in grass straws. J Agric Food Chem 43:2746–2751

Jung H, Mertens D, Payne A (1997) Correlation of acid detergent lignin and Klason lignin with digestibility of forage dry matter and neutral detergent fiber. J Dairy Sci 80:1622–1628

Kendall MG, Stuart A (1961) The advanced theory of statistics. In: Griffin C et al. (eds) Inference and relationship, vol 2, 3rd edn., London

Krakowsky M, Lee M, Beeghly H, Coors J (2003) Characterization of quantitative trait loci affecting fiber and lignin in maize (*Zea mays* L.). Maydica 48:283–292

Krakowsky M, Lee M, Coors J (2005) Quantitative trait loci for cell-wall components in recombinant inbred lines of maize (*Zea mays* L.). I: stalk tissue. Theor Appl Genet 111:337–346

Lander ES, Botstein D (1989) Mapping Mendelian factors underlying quantitative traits using RFLP linkage maps. Genetics 121:185–199

Legay S, Lacombe E, Goicoechea M, Briere C, Seguin A, MacKay J, Grima-Pettenati J (2007) Molecular characterization of EgMYB1, a putative transcriptional repressor of the lignin biosynthetic pathway. Plant Sci 173:542–549

Legay S, Sivadon P, Blervacq AS, Pavy N, Baghdady A, Tremblay L, Levasseur C, Ladouce N, Lapierre C, Séguin A, Hawkins S, Mackay J, Grima-Pettenati J (2010) EgMYB1, an R2R3 MYB transcription factor from eucalyptus negatively regulates secondary cell wall formation in Arabidopsis and poplar. New Phytol 188:774–786

Lundvall J, Buxton D, Hallauer A, George J (1994) Forage quality variation among maize inbreds: in vitro digestibility and cell-wall components. Crop Sci 34:1672–1678

Markussen T, Fladung M, Achere V, Favre JM, Faivre-Rampant P, Aragones A, Perez DD, Harvengt L, Espinel S, Ritter E (2003) Identification of QTLs controlling growth, chemical and physical wood property traits in Pinus pinaster (Ait.). Silvae Genetica 52:8–15

Martinez O, Curnow RN (1992) Estimating the locations and the sizes of the effects of quantitative trait loci using flanking markers. Theor Appl Genet 85:480–488

Parker G, Schofield R, Sundberg B, Turner S (2003) Isolation of COV1, a gene involved in the regulation of vascular patterning in the stem of Arabidopsis. Development 130:2139–2148

Pichon M, Deswartes C, Gerentes D, Guillaumie S, Lapierre C, Toppan A, Barrière Y, Goffner D (2006) Variation in lignin and cell wall digestibility in caffeic acid O-methyltransferase down-regulated maize half-sib progenies in field experiments. Mol Breed 18:253–261

Pires N, Dolan L (2010) Origin and diversification of basic-helix-loop-helix proteins in plants. Mol Biol Evol 27:862–874

Pot D, Rodrigues JC, Rozenberg P, Chantre G, Tibbits J, Cahalan C, Pichavant F, Plomion C (2006) QTLs and candidate genes for wood properties in maritime pine (Pinus pinaster Ait.). Tree Genet Genomes 2:10–24

Ralph J (2010) Hydroxycinnamates in lignification. Phytochem Rev 9:65–83

Ralph J, Helm RF, Quideau S, Hatfield RD (1992) Lignin feruloyl ester cross-links in grasses.1. Incorporation of feruloyl esters into coniferyl alcohol dehydrogenation polymers. J Chem Soc Perkin Trans 1:2961–2969

Ralph J, Grabber JH, Hatfield RD (1995) Lignin-ferulate cross-links in grasses—active incorporation of ferulate polysaccharide esters into ryegrass lignins. Carbohydr Res 275:167–178

Ramsay NA, Glover BJ (2005) MYB-bHLH-WD40 protein complex and the evolution of cellular diversity. Trends Plant Sci 10:63–70

Ranjan P, Yin T, Zhang X, Kalluri U, Yang X, Jawdy S, Tuskan G (2010) Bioinformatics-based identification of candidate genes from QTLs associated with cell wall traits in Populus. Bioenerg Res 3:172–182

Rengel D, San Clemente H, Servant F, Ladouce N, Paux E, Wincker P, Couloux A, Sivadon P, Grima-Pettenati J (2009) A new genomic resource dedicated to wood formation in *Eucalyptus*. BMC Plant Biol 9:36

Riboulet C, Lefèvre B, Denoue D, Barrière Y (2008) Genetic variation in maize cell wall for lignin content, lignin structure, *p*-hydroxycinnamic acid content, and digestibility in a set of 19 lines at silage harvest maturity. Maydica 53:11–19

Roussel V, Gibelin C, Fontaine AS, Barrière Y (2002) Genetic analysis in recombinant inbred lines of early dent forage maize. II-QTL mapping for cell wall constituents and cell wall digestibility from per se value and top cross experiments. Maydica 47:9–20

Sewell MM, Davis MF, Tuskan GA, Wheeler NC, Elam CC, Bassoni DL, Neale DB (2002) Identification of QTLs influencing wood property traits in loblolly pine (*Pinus taeda* L.). II. Chemical wood properties. TAG 104:214–222

Shi H, Kim YS, Guo Y, Stevenson B, Zhu JK (2003) The Arabidopsis SOS5 locus encodes a putative cell surface adhesion protein and is required for normal cell expansion. Plant Cell 15:19–32

Siefers N, Dang KK, Kumimoto RW, Bynum WE IV, Tayrose G, Holt BF III (2009) Tissue-specific expression patterns of Arabidopsis NF-Y transcription factors suggest potential for extensive combinatorial complexity. Plant Physiol 149:625–641

Sonbol FM, Fornalé S, Cappellades M, Encina A, Tourino S, Torres JL, Rovira P, Ruel K, Puigdomenech P, Rigau J, Caparros-Ruiz D (2009) The maize ZmMYB42 represses the phenylpropanoid pathway and affects the cell wall structure, composition and degradability in Arabidopsis thaliana. Plant Mol Biol 70:283–296

Struik P (1983) Physiology of forage maize (*Zea mays* L.) in relation to its production and quality. Ph. Dissertation, Agricultural University, 6700 GW Wageningen, The Netherlands, pp 1–252

Studer AJ, Doebley JF (2011) Do large effect QTL fractionate? A case study at the maize domestication QTL teosinte branched1. Genetics 188(3):673–681

Tamasloukht B, Wong-Quai-Lam S, Martinez Y, Tozo K, Barbier O, Jourda S, Jauneau A, Borderies G, Balzergue S, Renou JP, Martinant JP, Tatout C, Lapierre C, Barrière Y, Goffner D, Pichon M (2011) Characterization of a cinnamoyl-CoA reductase (CCR) mutant in maize: effects on lignification, fiber development, and global gene expression. J Exp Bot 62:3837–3848

Thimm O, Blasing O, Gibon Y, Nagel A, Meyer S, Kruger P, Selbig J, Muller LA, Rhee SY, Stitt M (2004) MAPMAN: a user-driven tool to display genomics data sets onto diagrams of metabolic pathways and other biological processes. Plant J 37:914–939

Thomas J, Guillaumie S, Verdu C, Denoue D, Pichon M, Barrière Y (2010) Cell wall phenylpropanoid-related gene expression in early maize recombinant inbred lines differing in parental alleles at a major lignin QTL position. Mol Breed 25:105–124

Thumma B, Southerton S, Bell J, Owen J, Henery M, Moran G (2010) Quantitative trait locus (QTL) analysis of wood quality traits in *Eucalyptus nitens*. Tree Genet Genomes 6:305–317

Utz H, Melchinger A (1996) PLABQTL: a program for composite interval mapping of QTL. J Agric Genomics 2:1–6

Schnable PS, Ware D, Fulton RS, Stein JC, Wei F, Pasternak S, Liang C, Zhang J, Fulton L, Graves TA, Minx P, Reily AD, Courtney

L, Kruchowski SS, Tomlinson C, Strong C, Delehaunty K, Fronick C, Courtney B, Rock SM, Belter E, Du F, Kim K, Abbott RM, Cotton M, Levy A, Marchetto P, Ochoa K, Jackson SM, Gillam B, Chen W, Yan L, Higginbotham J, Cardenas M, Waligorski J, Applebaum E, Phelps L, Falcone J, Kanchi K, Thane T, Scimone A, Thane N, Henke J, Wang T, Ruppert J, Shah N, Rotter K, Hodges J, Ingenthron E, Cordes M, Kohlberg S, Sgro J, Delgado B, Mead K, Chinwalla A, Leonard S, Crouse K, Collura K, Kudrna D, Currie J, He R, Angelova A, Rajasekar S, Mueller T, Lomeli R, Scara G, Ko A, Delaney K, Wissotski M, Lopez G, Campos D, Braidotti M, Ashley E, Golser W, Kim H, Lee S, Lin J, Dujmic Z, Kim W, Talag J, Zuccolo A, Fan C, Sebastian A, Kramer M, Spiegel L, Nascimento L, Zutavern T, Miller B, Ambroise C, Muller S, Spooner W, Narechania A, Ren L, Wei S, Kumari S, Faga B, Levy MJ, McMahan L, Van Buren P, Vaughn M,W, Ying K, Yeh C,-T, Emrich S,J, Jia Y, Kalyanaraman A, Hsia A-P, Barbazuk WB, Baucom RS, Brutnell TP, Carpita NC, Chaparro C, Chia J-M, Deragon J-M, Estill JC, Fu Y, Jeddeloh JA, Han Y, Lee H, Li P, Lisch DR, Liu S, Liu Z, Nagel DH, McCann MC, SanMiguel P, Myers AM, Nettleton D, Nguyen J, Penning BW, Ponnala L, Schneider KL, Schwartz DC, Sharma A, Soderlund C, Springer NM, Sun Q, Wang H, Waterman M, Westerman R, Wolfgruber TK, Yang L, Yu Y, Zhang L, Zhou S, Zhu Q, Bennetzen JL, Dawe RK, Jiang J, Jiang N, Presting GG, Wessler SR, Aluru S, Martienssen RA, Clifton SW, McCombie WR, Wing RA, Wilson RK (2009) The B73 maize genome: complexity, diversity, and dynamics. Science 326:1112–1115

Vignols F, Rigau J, Torres MA, Capellades M, Puigdomenech P (1995) The brown midrib3 (bm3) mutation in maize occurs in the gene encoding caffeic acid *O*-methyltransferase. Plant Cell 7:407–416

Wissenbach M, Uberlacker B, Vogt F, Becker D, Salamini F, Rohde W (1993) MYB genes from Hordeum vulgare—tissue-specific expression of chimeric MYB Promoter/Gus genes in transgenic tobacco. Plant J 4:411–422

Xu S (2003) Theoretical basis of the Beavis effect. Genetics 165:2259–2268

Yan J, Yang X, Shah T, Sánchez-Villeda H, Li J, Warburton M, Zhou Y, Crouch JH, Xu Y (2010) High-throughput SNP genotyping with the GoldenGate assay in maize. Mol Breed 25(3):441–451

Yang C, Xu Z, Song J, Conner K, Vizcay Barrena G, Wilson ZA (2007) Arabidopsis MYB26/MALE STERILE35 regulates secondary thickening in the endothecium and is essential for anther dehiscence. Plant Cell 19:534–548

Yin T, Zhang X, Gunter L, Priya R, Sykes R, Davis M, Wullschleger SD, Tuskan GA (2010) Differential detection of genetic Loci underlying stem and root lignin content in Populus. PLoS ONE 5(11):e14021

Zeng ZB (1994) Precision mapping of quantitative trait loci. Genetics 136:1457–1468

Zheng Z, Qamar SA, Chen Z, Mengiste T (2006) Arabidopsis WRKY33 transcription factor is required for resistance to necrotrophic fungal pathogens. Plant J 48:592–605